Electronic Supplementary Information

Experimental section

Materials: Vanadium(III) chloride (VCl_3), sodium sulfate (Na_2SO_4), ammonium chloride (NH_4Cl), terephthalic acid (H_2BDC), sodium citrate dehydrate ($C_6H_5Na_3O_7 \cdot 2H_2O$), *p*-dimethylaminobenzaldehyde ($C_9H_{11}NO$), sodium nitroferricyanide dihydrate ($C_5FeN_6Na_2O \cdot 2H_2O$), sodium hypochlorite solution (NaClO) and graphite powder were purchased from Aladdin Ltd. (Shanghai, China). Nafion (5 wt%) solution was purchased from Sigma-Aldrich Chemical Reagent Co., Ltd. Hydrochloric acid, nitric acid, sulfuric acid, hydrazine monohydrate ($N_2H_4 \cdot H_2O$) and ethyl alcohol (C_2H_5OH) were purchased from Kelong chemical Ltd. in Chengdu. The ultrapure water used throughout all experiments was purified through a Millipore system. All reagents were analytical reagent grade without further purification.

Preparation of V MOF and V_2O_3/C: V MOF was prepared according to the literature.[1] In a typical procedure, 314 mg of VCl_3 and 332 mg of terephthalic acid were mixed in a 50-mL beaker. Then, a solution containing 2 mL of HCl (1 $mol \cdot L^{-1}$) and 10 mL of absolute ethyl alcohol was added under vigorous stirring at room temperature. After 30 min, the resulting blue suspension was further dispersed with ultrasonic treatment for 15 min. Finally, the mixture was transferred to a 50-mL Teflon-lined stainless-steel autoclave and heated in an electrical oven at 120 °C for 2 day. The green powder, i.e., V MOF, were obtained via centrifugation with ethanol and dried in vacuum at 50 °C for 8 h. To obtain porous shuttlelike V_2O_3/C, the V MOF was annealed in Ar atmosphere at 700 °C for 6 h, with a heating rate of 2 $°C \cdot min^{-1}$.

Preparation of working electrode: CP was cleaned via brief sonication with ethanol and water for several times. To prepare the working electrode, 10 mg of the V_2O_3/C and 40 μL 5 wt% Nafion solution were dispersed in 960 μL water/ethanol (V : V = 1 : 2) followed by 1 h sonication to form a homogeneous ink. 20 μL of the catalyst suspension was loaded onto a CP (1 × 1 cm^2) and dried in Ar atmosphere at room temperature.

Characterizations: XRD patterns were performed using a LabX XRD-6100 X-ray

diffractometer with Cu Kα radiation (λ = 1.5418 Å) at 40 kV and 40 mA. SEM images were collected on a XL30 ESEM FEG scanning electron microscope at an accelerating voltage of 20 kV. The structures of the samples were determined by TEM images on a HITACHI H-8100 electron microscopy (Hitachi, Tokyo, Japan) operated at 200 kV. XPS measurements were performed on an ESCALABMK II X-ray photoelectron spectrometer using Mg as the exciting source. Raman spectra were obtained by a Renishaw inVia confocal Raman microprobe under 532 nm laser excitation. The absorbance data of spectrophotometer were measured on UV-Vis spectrophotometer. Thermal gravimetric analysis (TGA) was performed on a Perkin-Elmer Model Pyris1 TGA apparatus at a heating rate of 10 °C min^{-1} in air.

Electrochemical measurements: Electrochemical NRR measurements were performed in a two-compartment cell separated by Nafion 211 membrane using a CHI 660E electrochemical analyzer (CH Instruments, Inc.). The electrochemical experiments were carried out with a three-electrode configuration using graphite plate as the counter electrode and Ag/AgCl/saturated KCl as the reference electrode. In all measurements, saturated Ag/AgCl electrode was calibrated with respect to RHE as following: in 0.1 M Na_2SO_4 aqueous solution, E(RHE) = E(Ag/AgCl) + 0.059 × pH + 0.197 V. All experiments were carried out at room temperature (~ 25 °C). For N_2 reduction experiments, the Na_2SO_4 electrolyte (35 mL) was purged with N_2 for 30 min before the measurement. Pure N_2 was continuously fed into the cathodic compartment with a flow rate of 10 cm^3 min^{-1} during the experiments. The electrolyte itself was analyzed for detection of NH_3 before each potentiostatic test to ensure there was no contamination of NH_3 from the environment.

Determination of NH_3: 4 mL of sample was removed from the cathodic chamber, then added into 50 μL of oxidizing solution containing NaClO (ρ_{Cl} = 4~4.9) and NaOH (0.75 M), then added 500 μL coloring solution containing 0.4 M $C_6H_5Na_3O_7 \cdot 2H_2O$ and 0.32 M NaOH and 50 μL catalyst solution (0.1 g $Na_2[Fe(CN)_5NO] \cdot 2H_2O$ diluted to 10 ml with deionized water) in turn. Absorbance measurements were performed after one hour at λ = 660 nm. The calibration curve (y = 0.734x + 0.013, R^2=0.999) shows good linear relation of absorbance value with NH_3 concentration by three times

independent calibrations.

NH_3 yield was calculated using the following equation: NH_3 yield = (c_{NH3} × V) / (t × m). FE was calculated according to following equation: FE = 3 × F × c_{NH3} × V / (17 × Q), where c_{NH3} is the measured NH_3 concentration, V is the volume of the cathodic reaction electrolyte, t is the reduction reaction time, m is the catalyst mass, F is the Faraday constant, and Q is the quantity of applied electricity.

Determination of N_2H_4: A mixture of p-$C_9H_{11}NO$ (5.99 g), HCl (concentrated, 30 mL) and C_2H_5OH (300 mL) was used as a color reagent. In detail, 5 mL electrolyte was removed from the electrochemical reaction vessel, and added into 5 mL above prepared color reagent and stirring 10 min at room temperature. The absorbance of the resulting solution was measured at 455 nm. The calibration curve ($y = 0.397x + 0.032$, $R^2 = 0.999$) shows good linear relation of absorbance value with N_2H_4 concentration by three times independent calibrations.

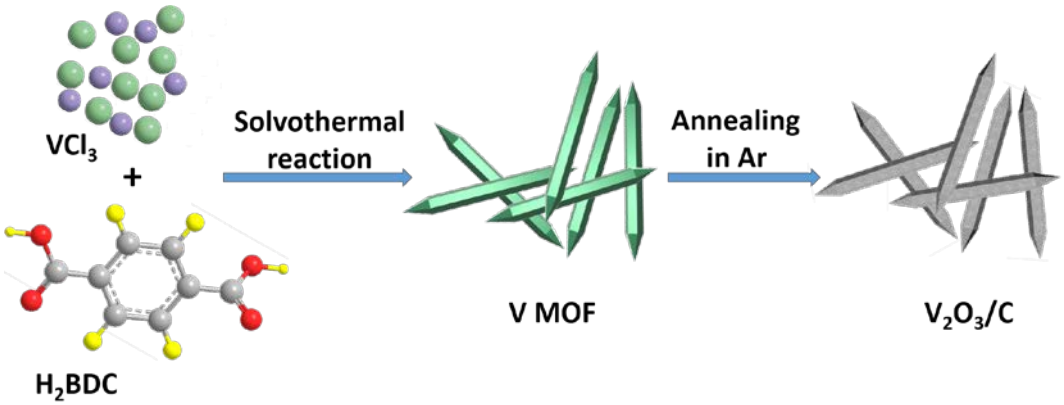

Scheme S1. Illustration of preparation process for shuttle-like V_2O_3/C.

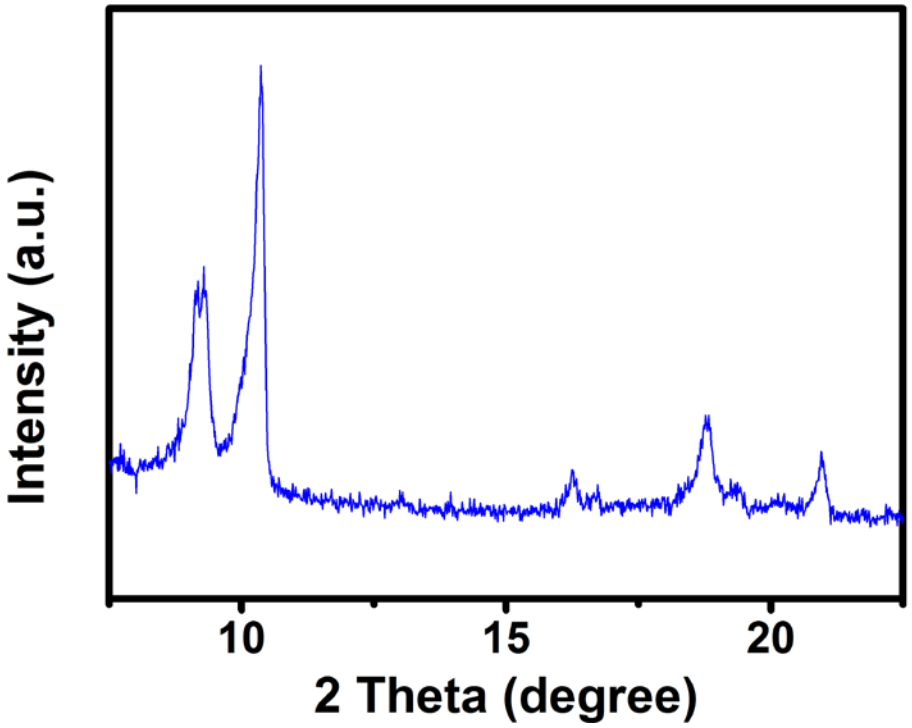

Fig. S1. XRD pattern of V MOF.

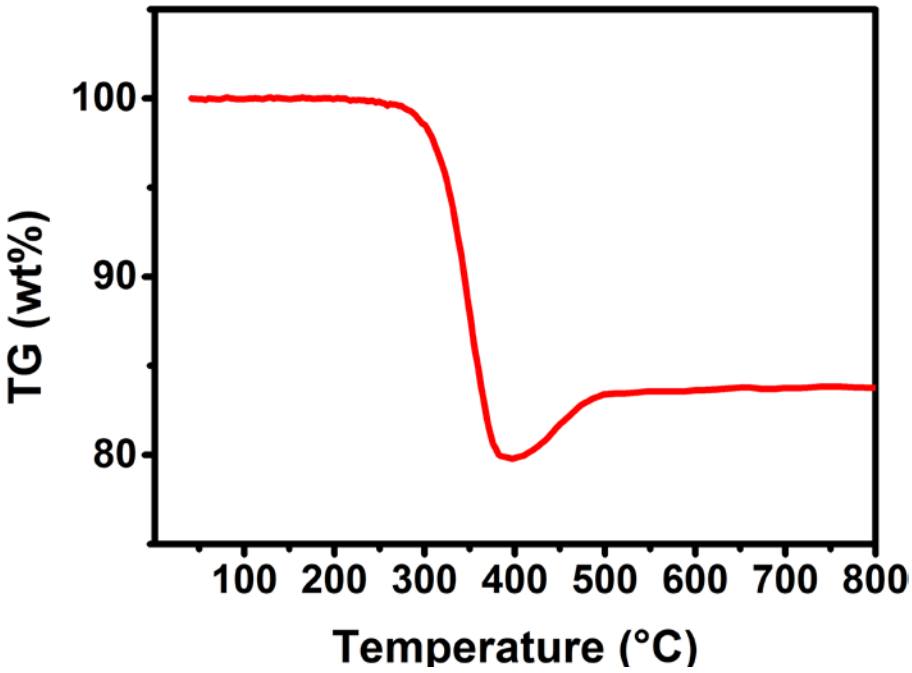

Fig. S2. TGA curve of V_2O_3/C.

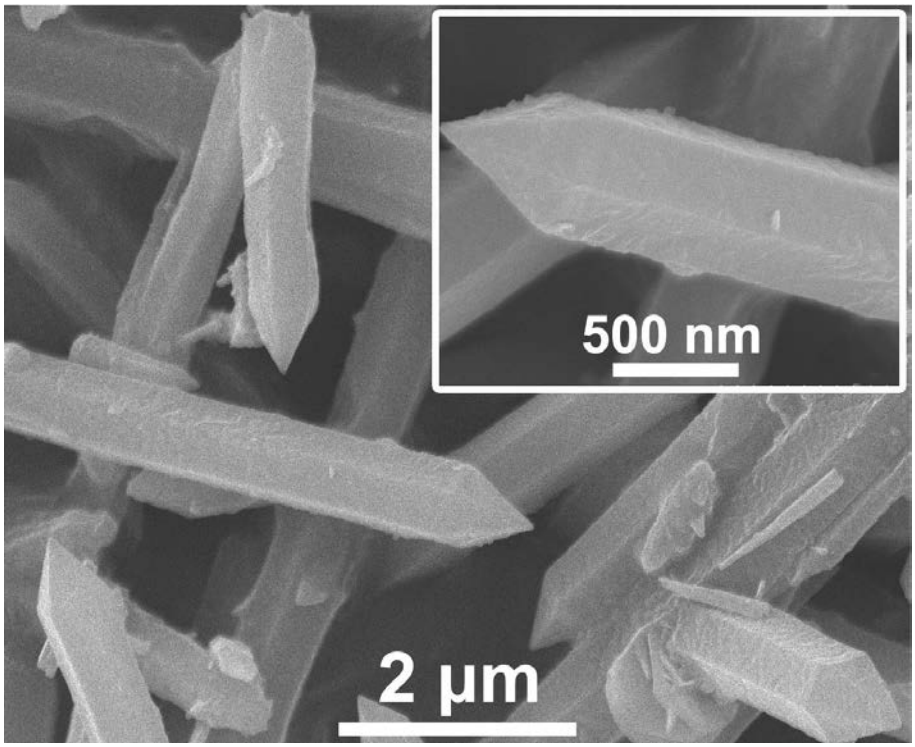

Fig. S3. SEM images of V MOF.

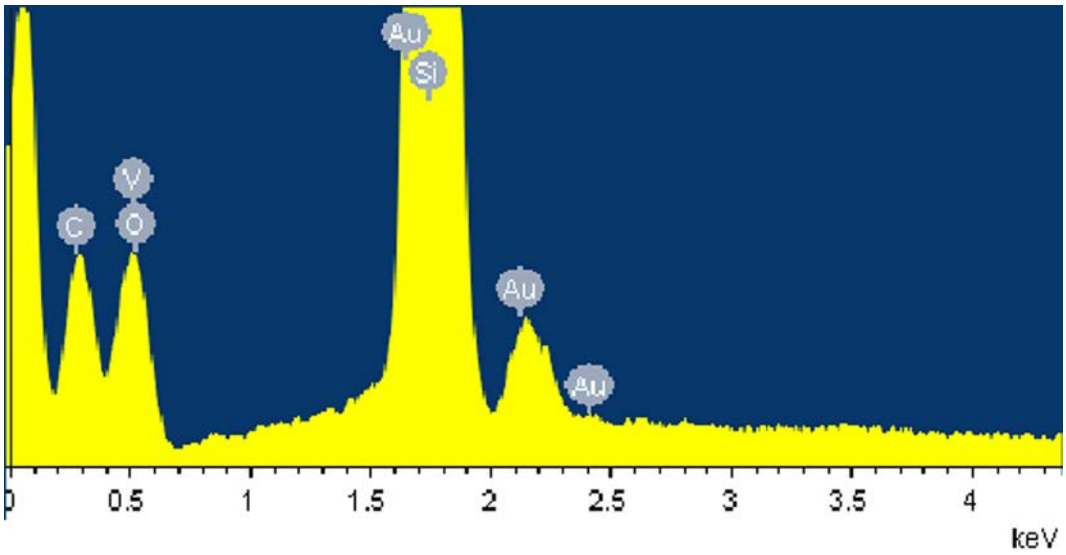

Fig. S4. EDX spectrum of V_2O_3/C (note: Au signal arises from the sprayed Au species on the sample surface to enhance the conductivity for SEM and EDX characterizations; Si signal arises from the Si substrate).

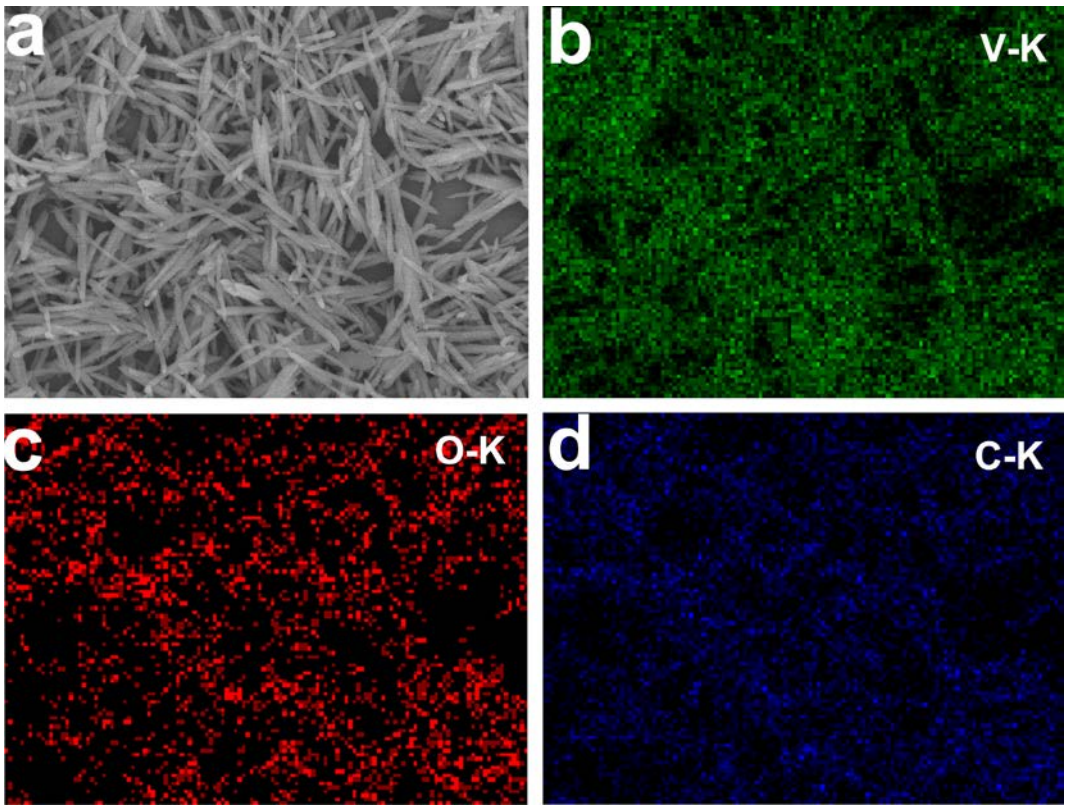

Fig. S5. (a) SEM image and EDX elemental mapping images of (b) V, (c) O, and (d) C elements in V_2O_3/C.

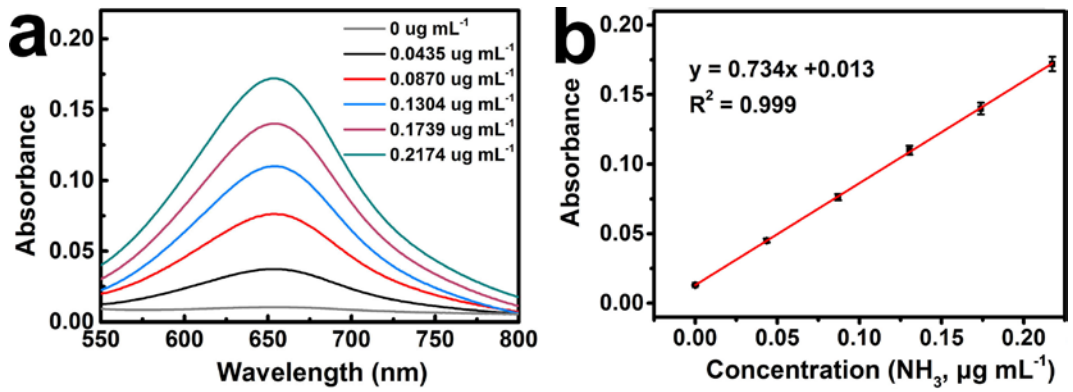

Fig. S6. (a) UV-Vis absorption spectra of indophenol assays with different NH_4^+ concentrations after incubated for 2 h at room temperature. (b) Calibration curve used for calculation of NH_3 concentrations.

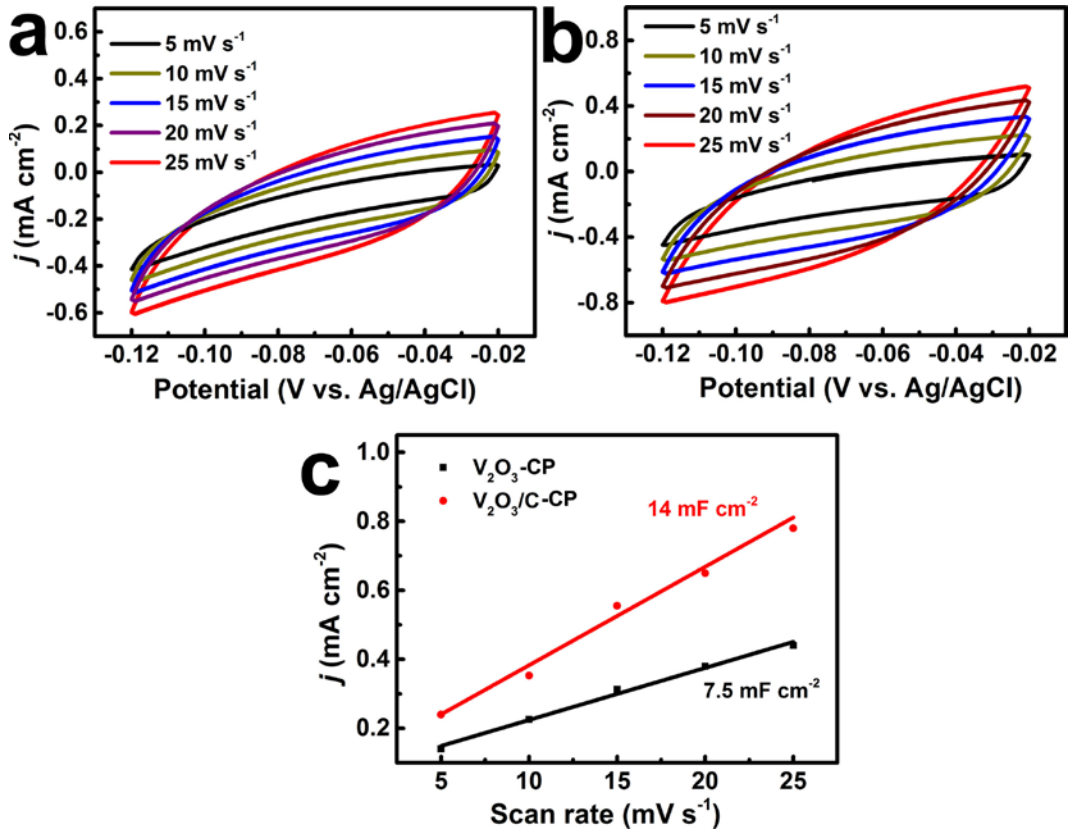

Fig. S7. Cyclic voltammetry curves of (a) V_2O_3/C-CP and (b) V_2O_3-CP with various scan rates in the region of –0.02 to –0.12 V vs. Ag/AgCl. (c) The capacitive current densities at –0.07 V vs. Ag/AgCl as a function of scan rates for V_2O_3/C-CP and V_2O_3-CP.

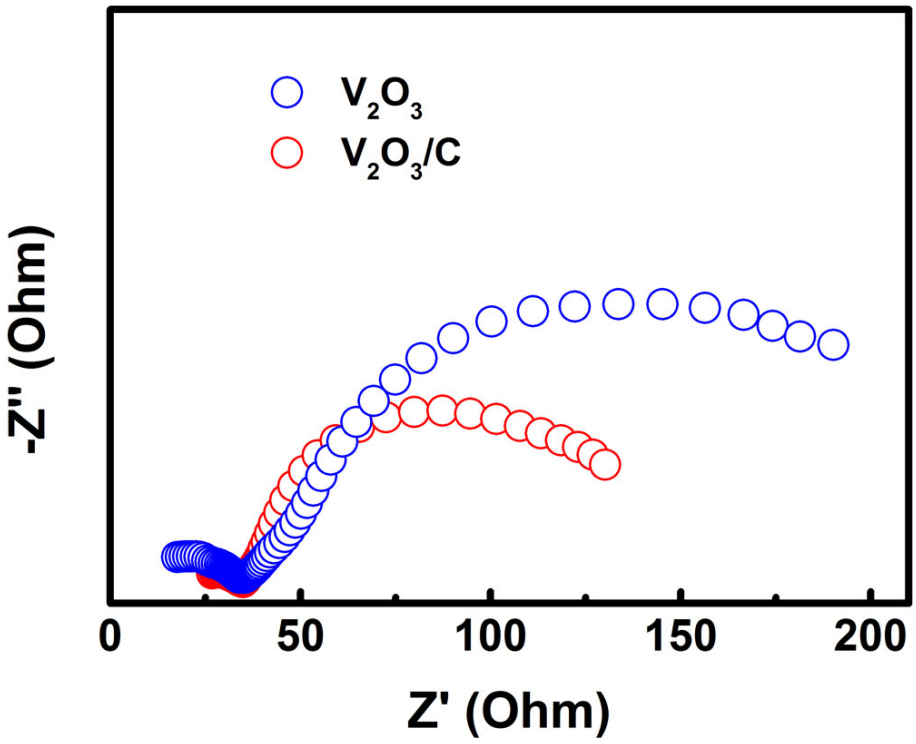

Fig. S8. Nyquist plots of V_2O_3/C-CP and V_2O_3-CP at open circuit potential.

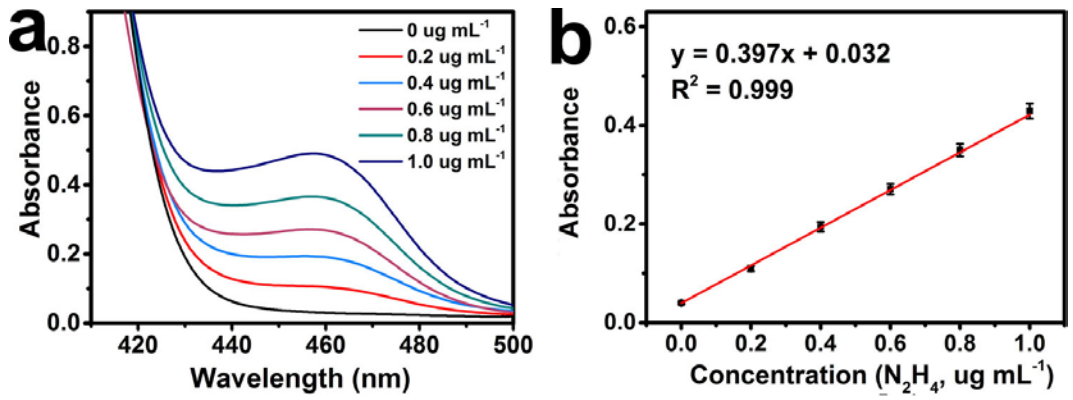

Fig. S9. UV-Vis absorption spectra of various N_2H_4 concentrations after incubated for 10 min at room temperature. (b) Calibration curve used for calculation of N_2H_4 concentrations.

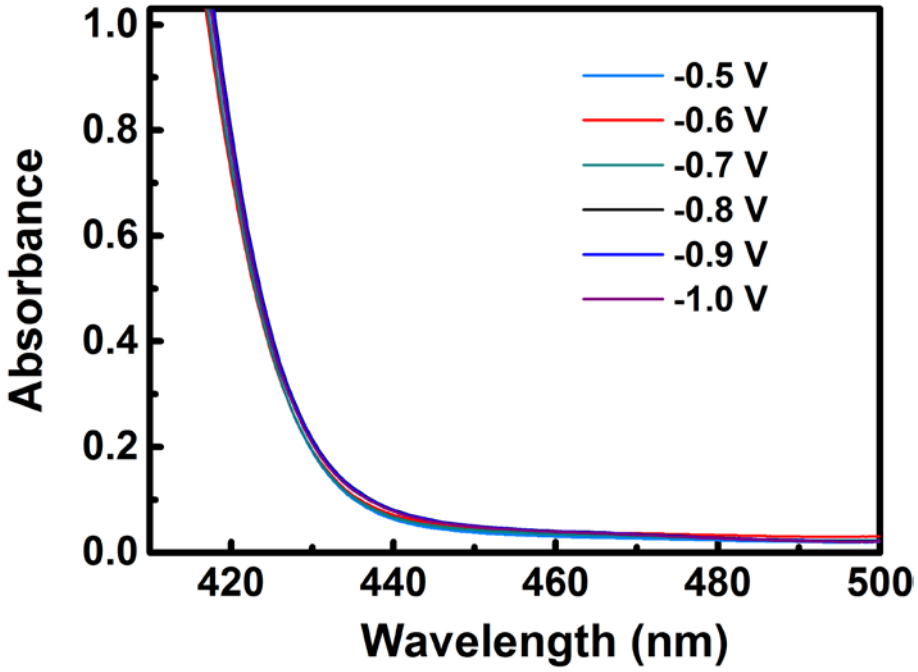

Fig. S10. UV-Vis absorption spectra of electrolytes stained with p-$C_9H_{11}NO$ after 2-h electrolysis at different potentials using post-NRR V_2O_3/C-CP.

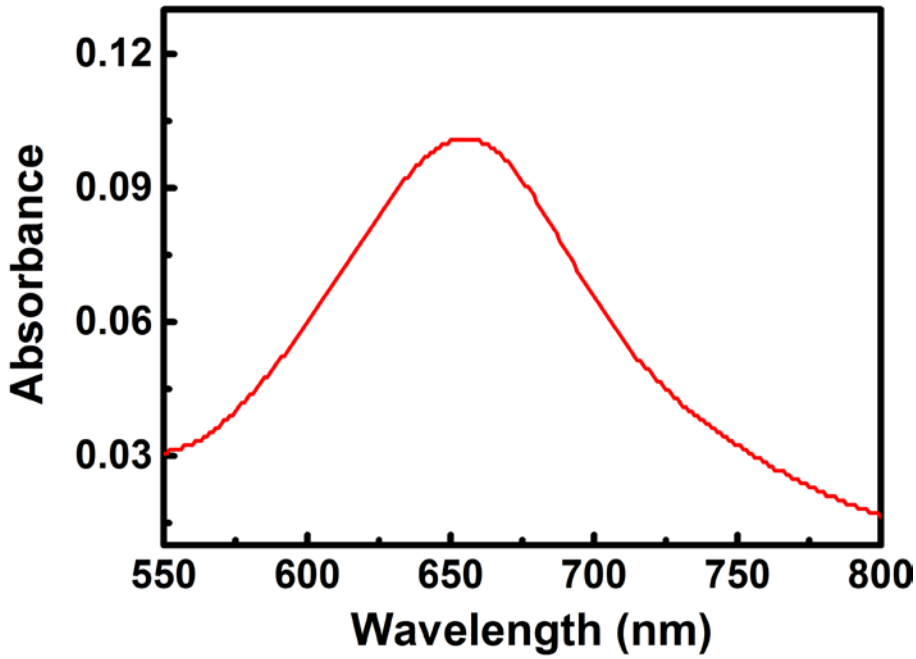

Fig. S11. UV-Vis absorption spectra of electrolyte stained with indophenol indicator after 2-h potentiostatic test at –0.6 V using post-NRR V_2O_3/C-CP.

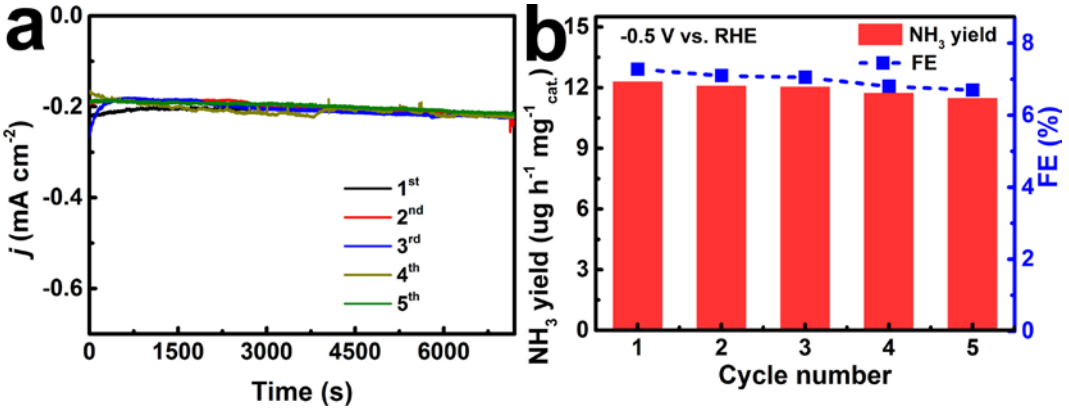

Fig. S12. (a) Chronoamperometric curves of V_2O_3/C-CP at –0.6 V for 5 times. (b) NH_3 yields and FEs of V_2O_3/C-CP at –0.6 V for 5 cycles.

Fig. S13. Photograph of pH test papers of electrolytes before (left) and after (right) electrolysis.

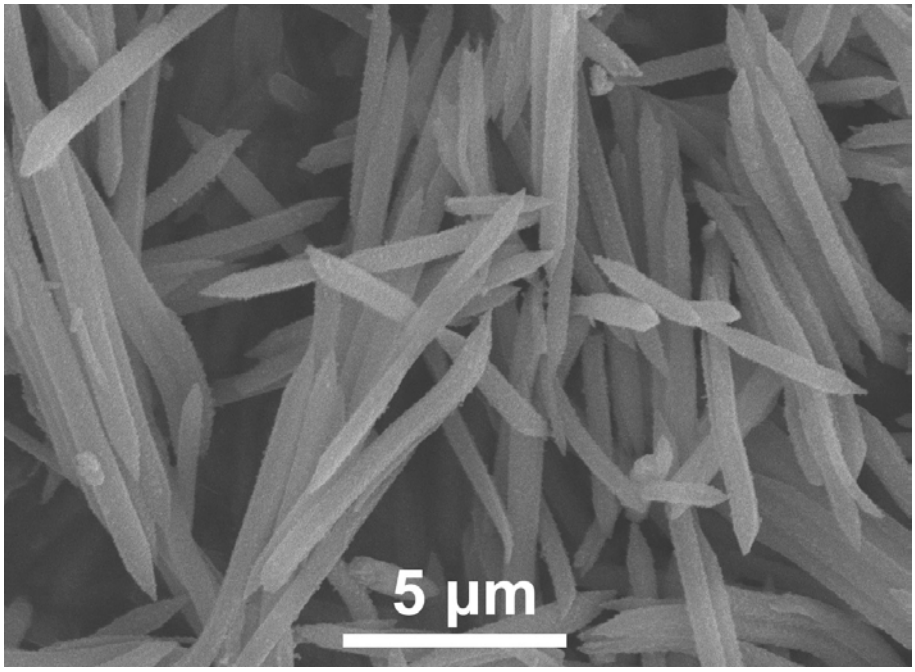

Fig. S14. SEM image of post-NRR V_2O_3/C.

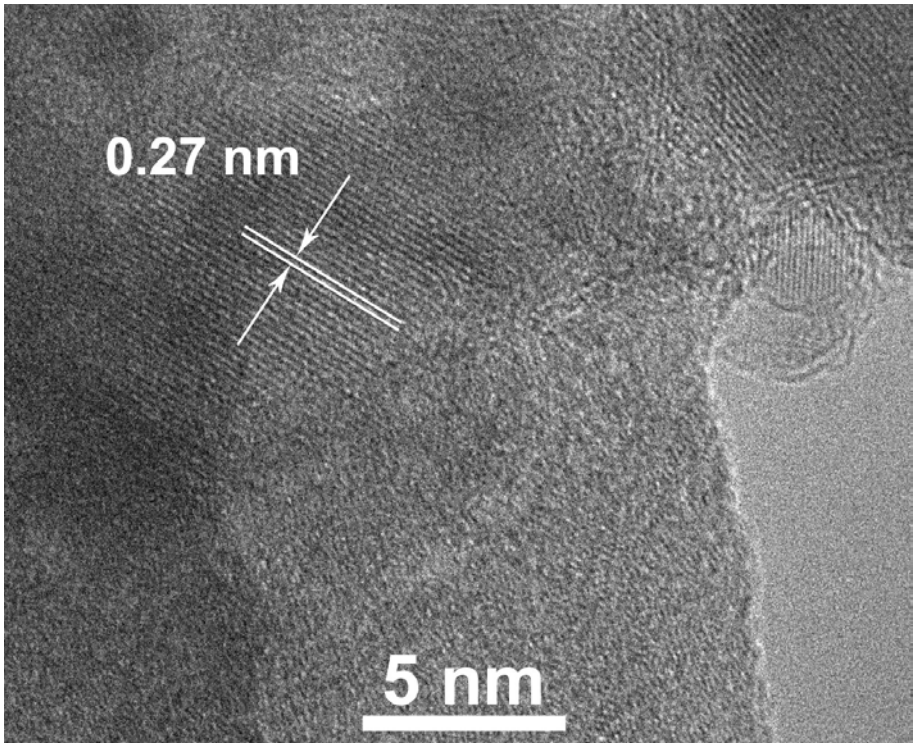

Fig. S15. HRTEM image of post-NRR V_2O_3/C.

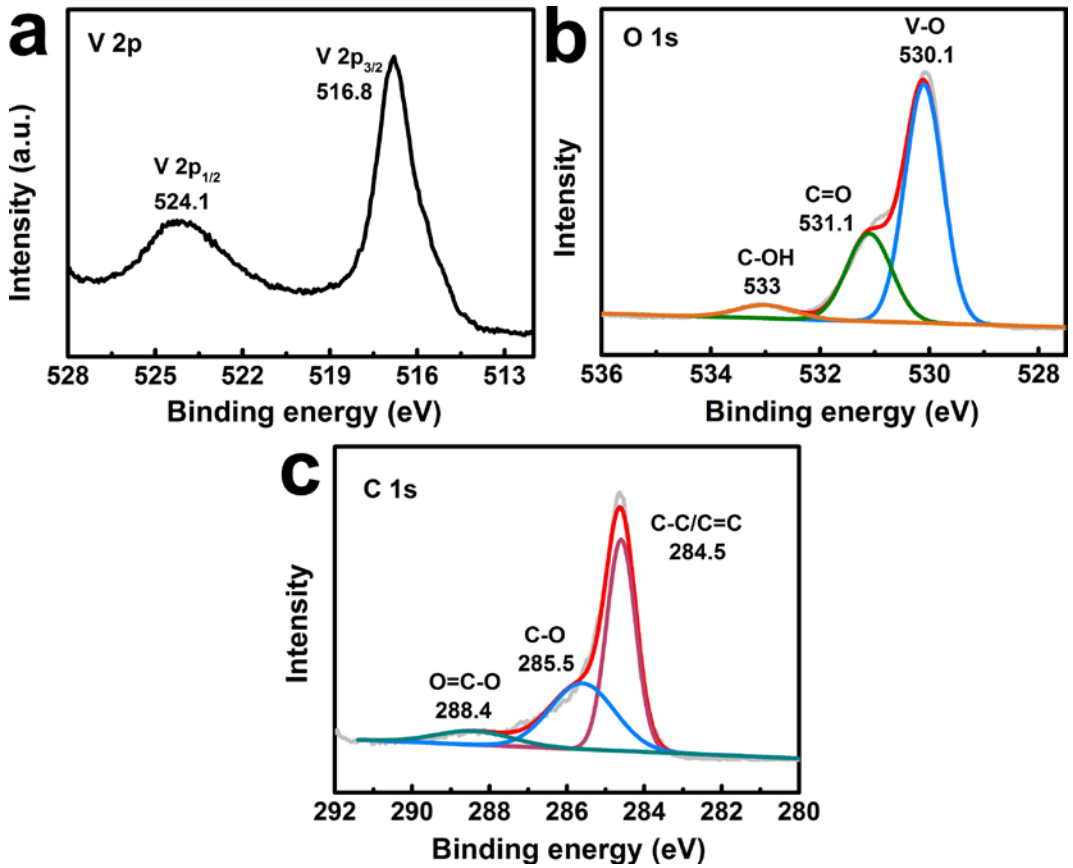

Fig. S16. XPS spectra of post-NRR V_2O_3/C in the (a) V 2p, (b) O 1s, and (c) C 1s regions.

Table S1. The values of Q at different potentials obtained from the potentiostat.

Potential (V)	Q (C)
–0.5	0.72
–0.6	1.152
–0.7	1.512
–0.8	2.1924
–0.9	4.68
–1	11.052

Table S2. Comparison of electrocatalytic NRR performance for V_2O_3/C with other electrocatalysts under ambient conditions.

Catalyst	Electrolyte	NH_3 yield	FE (%)	Ref.
V_2O_3/C	**0.1 M Na_2SO_4**	**12.3 μg h^{-1} $mg^{-1}_{cat.}$ (2.46 μg h^{-1} cm^{-1})**	**7.28**	**This work**
α-Au/CeO_x-RGO	0.1 M HCl	8.31 μg h^{-1} $mg^{-1}_{cat.}$	10.1	2
TA-reduced Au/TiO_2	0.1 M HCl	21.4 μg h^{-1} $mg^{-1}_{cat.}$	8.11	3
Au nanorods	0.1 M KOH	1.6 μg h^{-1} cm^{-2}	3.88	4
Rh	0.1 M KOH	23.88 μg h^{-1} $mg^{-1}_{cat.}$	0.217	5
$Pd_{0.2}Cu_{0.8}$/rGO	0.1 M KOH	2.8 μg h^{-1} $mg^{-1}_{cat.}$	4.5	6
Pd/C	0.1M PBS	4.5 μg h^{-1} $mg^{-1}_{cat.}$	8.2	7
PEBCD/C	0.5 M Li_2SO_4	1.58 μg h^{-1} cm^{-2}	2.85	8
γ-Fe_2O_3	0.1 M KOH	0.212 μg h^{-1} $mg^{-1}_{cat.}$	1.9	9
Fe_2O_3-CNT	$KHCO_3$	0.22 μg h^{-1} cm^{-2}	0.15	10
Fe_3O_4/Ti	0.1 M Na_2SO_4	3.43 μg h^{-1} cm^{-1}	2.60	11
Mo nanofilm	0.01 M H_2SO_4	1.89 μg h^{-1} cm^{-2}	0.72	12
MoO_3	0.1 M HCl	29.43 μg h^{-1} $mg^{-1}_{cat.}$	1.9	13
MoS_2/CC	0.1 M Na_2SO_4	4.94 μg h^{-1} cm^{-2}	1.17	14
N-doped porous carbon	0.05 M H_2SO_4	23.8 μg h^{-1} $mg^{-1}_{cat.}$	1.42	15
N-doped porous carbon	0.1 M HCl	15.7 μg h^{-1} $mg^{-1}_{cat.}$	1.45	16
Mo_2N	0.1 M HCl	78.4 μg h^{-1} $mg^{-1}_{cat.}$	4.5	17
MoN	0.1 M HCl	18.42 μg h^{-1} cm^{-2}	1.15	18
VN	0.1 M HCl	5.14 μg h^{-1} cm^{-2}	2.25	19
$Bi_4V_2O_{11}$/CeO_2	0.1 M HCl	23.21 μg h^{-1} $mg^{-1}_{cat.}$	10.16	20
TiO_2 nanosheets	0.1 M Na_2SO_4	5.6 μg h^{-1} cm^{-2}	2.50	21

Multishelled hollow Cr_2O_3 microspheres	0.1 M Na_2SO_4	25.3 μg h^{-1} $mg^{-1}_{cat.}$	6.78	22
B_4C	0.1 M HCl	26.57 μg h^{-1} $mg^{-1}_{cat.}$	15.95	23

References

1 D Y. Cai, G. Fang, J. Zhou, S. Liu, Z. Luo, A. Pan, G. Cao and S. Liang, *Nano Res.*, 2018, **11**, 449–463.

2 S. Li, D. Bao, M. Shi, B. Wulan, J. Yan and Q. Jiang, *Adv. Mater.*, 2017, **29**, 1700001.

3 M. Shi, D. Bao, B. Wulan, Y. Li, Y. Zhang, J. Yan and Q. Jiang, *Adv. Mater.*, 2017, **29**, 1606550.

4 D. Bao, Q. Zhang, F. Meng, H. Zhong, M. Shi, Y. Zhang, J. Yan and Q. Jiang and X. Zhang, *Adv. Mater.*, 2017, **29**, 1604799.

5 H. Liu, S. Han, Y. Zhao, Y. Zhu, X. L. Tian, J. Zeng, J. Jiang, B. Y. Xia and Y. Chen, *J. Mater. Chem. A*, 2018, **6**, 3211–3217.

6 M. Shi, D. Bao, S. Li, B. Wulan, J. Yan and Q. Jiang, *Adv. Energy Mater.*, 2018, **8**, 1800124.

7 J. Wang, L. Yu, L. Hu, G. Chen, H. Xin and X. Feng, *Nat. Commun.*, 2018, **9**, 1795.

8 G. Chen, X. Cao, S. Wu, X. Zeng, L. Ding, M. Zhu and H. Wang, *J. Am. Chem. Soc.*, 2017, **139**, 9771–9774.

9 J. Kong, A. Lim, C. Yoon, J. H. Jang, H. C. Ham, J. Han, S. Nam, D. Kim, Y.-E. Sung, J. Choi and H. S. Park, *ACS Sustainable Chem. Eng.*, 2017, **5**, 10986–10995.

10 S. Chen, S. Perathoner, C. Ampelli, C. Mebrahtu, D. Su and G. Centi, *Angew. Chem., Int. Ed.*, 2017, **56**, 2699–2703.

11 Q. Liu, X. Zhang, B. Zhang, Y. Luo, G. Cui, F. Xie and X. Sun, *Nanoscale*, 2018, **10**, 14386–14389.

12 D. Yang, T. Chen and Z. Wang, *J. Mater. Chem. A*, 2017, **5**, 18967–18971.

13 J. Han, X. Ji, X. Ren, G. Cui, L. Li, F. Xie, H. Wang, B. Li and X. Sun, *J. Mater. Chem. A*, 2018, **6**, 12974–12977.

14 L. Zhang, X. Ji, X. Ren, Y. Ma, X. Shi, Z. Tian, A. M. Asiri, L. Chen, B. Tang and X. Sun, *Adv. Mater.*, 2018, **30**, 1800191.

15 Y. Liu, Y. Su, X. Quan, X. Fan, S. Chen, H. Yu, H. Zhao, Y. Zhang and J. Zhao, *ACS Catal.*, 2018, **8**, 1186−1191.

16 X. Yang, K. Li, D. Cheng, W. Pang, J. Lv, X. Chen, H. Zang, X. Wu, H. Tan, Y. Wang and Y. Li, *J. Mater. Chem. A*, 2018, **6**, 7762–7769.

17 X. Ren, G. Cui, L. Chen, F. Xie, Q. Wei, Z. Tian and X. Sun, *Chem. Commun.*, 2018, **54**, 8474–8477.

18 L. Zhang, X. Ji, X. Ren, Y. Luo, X. Shi, A. M. Asiri, B. Zheng and X. Sun, *ACS Sustainable Chem. Eng.*, 2018, **6**, 9550–9554.

19 R. Zhang, Y. Zhang, X. Ren, G. Cui, A. M. Asiri, B. Zheng and X. Sun, *ACS Sustainable Chem. Eng.*, 2018, **6**, 9545–9549.

20 C. Lv, C. Yan, G. Chen, Y. Ding, J. Sun, Y. Zhou and G. Yu, *Angew. Chem., Int. Ed.*, 2018, **57**, 6073–6076.

21 R. Zhang, X. Ren, X. Shi, F. Xie. B. Zheng, X. Guo and X. Sun, *ACS Appl. Mater. Interfaces*, 2018, **10**, 28251–28255.

22 Y. Zhang, W. Qiu, Y. Ma, Z. Tian, G. Cui, F. Xie, L. Chen, T. Li and X. Sun, *ACS Catal.*, 2018, **8**, 8540–8544.

23 W. Qiu, X. Xie, J. Qiu, W. Fang, R. Liang, X. Ren, X. Ji, G. Cui, A. M. Asiri, G. Cui, B. Tang and X. Sun, *Nat. Commun.*, 2018, **9**, 3485.